Fuel 242 (2019) 624–637

Contents lists available at ScienceDirect

Fuel

journal homepage: www.elsevier.com/locate/fuel

Full Length Article

Dynamic behavior investigations and disturbance rejection predictive control of solvent-based post-combustion CO_2 capture process

Xiao Wu[a,*], Jiong Shen[a], Yiguo Li[a], Meihong Wang[b,*], Adekola Lawal[c], Kwang Y. Lee[d]

[a] Key Laboratory of Energy Thermal Conversion and Control of Ministry of Education, Southeast University, Nanjing 210096, China
[b] Department of Chemical and Biological Engineering, The University of Sheffield, Sheffield S1 3JD, UK
[c] Process Systems Enterprise Ltd, 26-28 Hammersmith Grove, London W6 7HA, UK
[d] Department of Electrical and Computer Engineering, Baylor University, One Bear Place #97356, Waco, TX 76798-7356, USA

GRAPHICAL ABSTRACT

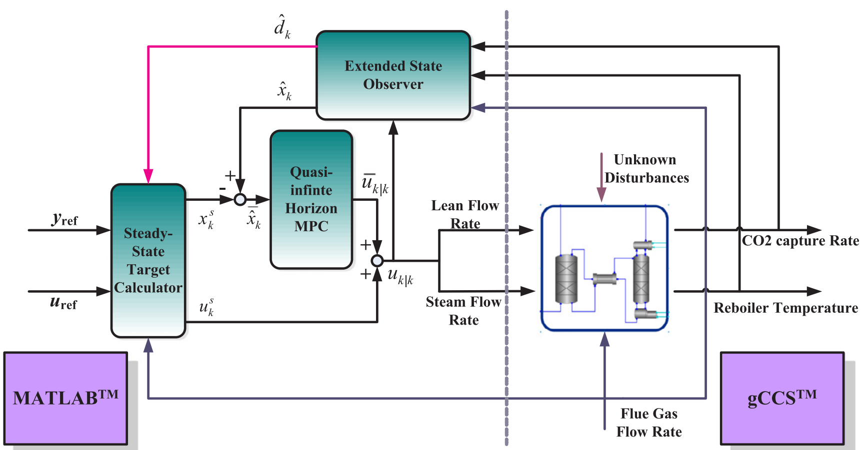

ARTICLE INFO

Keywords:
Post-combustion carbon capture
Chemical absorption
Flexible operation
Dynamic behavior variations
Model predictive control
Disturbance rejection

ABSTRACT

Increasing demand for flexible operation has posed significant challenges to the control system design of solvent-based post-combustion CO_2 capture (PCC) process: 1) the capture system itself has very slow dynamics; 2) in the case of wide range of operation, dynamic behavior of the PCC process will change significantly at different operating points; and 3) the frequent variation of upstream flue gas flowrate will bring in strong disturbances to the capture system. For these reasons, this paper provides a comprehensive study on the dynamic characteristics of the PCC process. The system dynamics under different CO_2 capture rates, re-boiler temperatures, and flue gas flow rates are analyzed and compared through step-response tests. Based on the in-depth understanding of the system behavior, a disturbance rejection predictive controller (DRPC) is proposed for the PCC process. The predictive controller can track the desired CO_2 capture rate quickly and smoothly in a wide operating range while tightly maintaining the re-boiler temperature around the optimal value. Active disturbance rejection approach is used in the predictive control design to improve the control property in the presence of dynamic variations or disturbances. The measured disturbances, such as the flue gas flow rate, is considered as an additional input in the predictive model development, so that accurate model prediction and timely control adjustment can be made once the disturbance is detected. For unmeasured disturbances, including model

* Corresponding authors.
E-mail addresses: wux@seu.edu.cn (X. Wu), Wang@sheffield.ac.uk (M. Wang).

https://doi.org/10.1016/j.fuel.2019.01.075
Received 30 May 2018; Received in revised form 14 November 2018; Accepted 9 January 2019
0016-2361/

mismatches, plant behavior variations, etc., a disturbance observer is designed to estimate the value of disturbances. The estimated signal is then used as a compensation to the predictive control signal to remove the influence of disturbances. Simulations on a monoethanolamine (MEA) based PCC system developed on gCCS demonstrates the excellent effect of the proposed controller.

1. Introduction

Massive anthropogenic emissions of carbon dioxide is viewed as the main cause of global warming [1]. More than 30% of these emissions has the origin from fossil-fuel fired power plants, especially coal-fired power plants, which are the dominant devices in the power industry [2]. Therefore, CO_2 capture of coal-fired power plants is of great importance for mitigating global warming, greenhouse effect and related issues [3].

Many in-depth studies have been conducted for the carbon capture technology. Among them, chemical absorption based post-combustion CO_2 capture (PCC) is mature in technology and the installation of PCC devices requires only little modification to the existing power units. For these reasons, the PCC technology has been regarded as the most promising approach for the CO_2 removal of coal-fired power plants [3]. However, the high energy consumption required for solvent regeneration becomes barrier to its large-scale commercial deployment. To develop an efficient process for CO_2 separation from power plant flue gas, many studies on solvent selection [4–7], process configuration [8–10], parameter settings [6,7] have been undertaken. These studies only focused on the steady-state optimization at a full operating condition.

In recent years, there has been an increasing demand on the flexible operation of PCC processes [11–20]. From external perspectives, with the extensive penetration of renewable energy in the power grid, the coal-fired power plants have to change their loading rapidly over a wide range to alleviate the impact of unstable renewable power supplies and varying load demand [21]. As a result, the flue gas flow rate will have significant variations. In this regard, the PCC plants are forced to operate in a flexible manner and follow these changes [12]. On the other hand, from internal perspectives, flexible operation is also a requirement for the PCC process itself, because flexible adjustment of CO_2 capture rate is the foundation for the entire power generation-carbon capture system to achieve a better scheduling considering the demands of power generation, energy consumption, system efficiency and carbon emission [12].

In this context, thorough understanding of the dynamic characteristics of the PCC system over the entire operating range and design of appropriate control system for the process have become emerging and concerned topics.

Establishing accurate dynamic PCC models and conducting experiments with the models is the most important step to understand system characteristics. Lawal et al. [22] investigated the dynamics of the standalone absorber based on dynamic modeling of the process. Their studies indicated that maintaining the ratio between lean solvent flow rate and flue gas flow rate is vital for partial load operation of the absorber. Their findings also showed that the CO_2 loading of lean solvent had significant impact on the performance of the absorber. Ziaii et al. [23] developed a rate-based dynamic model for the CO_2 stripper system. Besides carrying out steady-state optimizations, the dynamic variation of steam rate and rich solvent rate, and their influence on the stripper performance were also investigated. In order to understand the dynamic behavior of the entire capture system, detailed analytical models composed by a series of mathematical equations are established based on a variety of simulation platforms, such as gPROMS [11,12], Aspen Dynamics [15,16], Modelica [24,25], Matlab [26] and gCCS [27,28]. The dynamic effects of solvent circulation rate, flue gas flow rate/composition and re-boiler heat duty on the key variables of the capture system were then studied through simulation on these models. In [29–31], data-driven identification models such as bootstrap aggregated neural network model [29], nonlinear auto-regressive exogenous (NLARX) model [30] and neural fuzzy model [31] were developed for the solvent-based PCC system. Compared with the conventional first principle modeling approach, which needs a thorough understanding of the capture process and equipment design specifications, dynamic operation data is the only requirement for these models.

In [32] and [19], open-loop step response tests were carried out respectively at Esbjerg pilot plant and AGL Loy Yang power station to gain practical experience for the dynamic behavior of the PCC process. The parameters studied include flue gas flow rate, solvent flow rate and re-boiler duty. The experimental results showed the slow dynamics of the entire capture system and the strong couplings among multi-variables.

In Montañés et al. [25], dynamic model of a 600 MWe combined-cycle power plant with post-combustion CO_2 capture was developed using Modelica. The step response tests of the PCC system were then conducted at 100%, 80% and 60% gas turbine load. The results showed that at lower gas turbine loading condition, the dynamics of PCC system was slower. In addition, they found that the plant responses corresponding to the increase or decrease of a certain variable were different.

The researches on the dynamic characteristics effectively provide directions for the control system design of the PCC process. Based on the results, a general control structure was proposed and used in [12,15,16,33–37], which involved four key variables: the CO_2 capture rate, the re-boiler temperature, the lean solvent flow rate and the re-boiler heat duty. In most of these studies, 2-input 2-output decentralized proportional-integral (PI) control systems were designed, which used the lean solvent flow rate to adjust the CO_2 capture rate, and the re-boiler heat duty to adjust the re-boiler temperature. The simulations demonstrated that such a design could achieve a prompt control for the CO_2 capture rate and effectively alleviate the disturbances of the inlet flue gas flow rate and concentration variations. To maintain a better hydraulic stability of the absorber and stripper column, in Lin et al. [16], the lean solvent flow rate was fixed at a given value, and the re-boiler steam flow rate, which can change the lean solvent loading was selected to control the CO_2 capture rate.

Nittaya et al. [36] presented three decentralized PI control structures for the PCC process: 1) using the relative gain array (RGA) to pair the control loop; 2) heuristic approach using lean solvent flow rate to control the capture rate, and re-boiler heat duty to control the re-boiler temperature; and 3) heuristic approach using rich solvent flow rate to control the re-boiler temperature, and re-boiler heat duty to control the capture rate. Simulation results under different cases such as flue gas flow rate variation and set-point tracking showed that under normal working condition, the second control structure had the best performance. Authors then extended the pilot-scale PCC model to a commercial-scale model that matched a 750MWe coal-fired power plant using gPROMS [37]. The dynamic performance under the second control structure was evaluated through simulations. The results revealed that, the PCC plant was able to reject various disturbances and switch promptly between different operating points.

Panahi and Skogestad [33,34] divided the operation range of PCC system into three regions according to the flue gas flow rate of upstream power plant while considering the limitation of re-boiler heat duty. Steady-state optimizations were conducted for each region considering the energy consumption and penalty of CO_2 emission. The variables that were most closely related to the optimization performance were selected as controlled variables. Five control alternatives (four decentralized PI control structures and one multi-variable model predictive control structure) were then presented and the simulation results showed that the most advantageous PI control system was comparable to the predictive controller in the presence of large flue gas flow rate variation.

In order to better respond to the changes of flue gas flow rate, in [22] and [38], the idea of feed-forward control was applied to the PCC process control design. The solvent flow rate was required to vary synchronously with the flue gas flow rate (i.e., maintaining the L/G ratio) and the simulations demonstrated that such a design was more beneficial for attaining a designed CO_2 capture rate control.

Besides conventional PI controls, in recent years, a number of researchers have used the approach of model predictive control (MPC) for the capture process [13,14,17,18,35,39–46]. The basic idea of MPC is to use an explicit process model to predict the future response of the plant and calculate the control inputs through the minimization of a dynamic objective function within the prediction horizon. Because of the MPC's natural advantages in handling multi-variable, slow dynamic, constrained system, better performance has been reported in the PCC controller design, compared to the PI control structures.

Due to the strong nonlinearity of the PCC system, [41] and [42] directly used the simplified nonlinear analytical model as the predictive model and designed nonlinear MPCs for the flexible operation of the PCC plant. The monoethanolamine (MEA) recirculation rate and re-boiler heat flow were considered as the manipulated variables. The simulation results on Modelica platform showed that the target CO_2 removal efficiency could be quickly tracked by the proposed nonlinear MPC in a wide operation range. Zhang et al. [43] identified a nonlinear additive autoregressive model with exogenous variables (NAARX model) as the predictive model, and developed a nonlinear MPC for the PCC process. Fast tracking performance can be achieved by the nonlinear MPC under wide changes in power load and CO_2 capture rate. However, the use of nonlinear MPC requires solving large-scale nonlinear dynamic optimization problems, which is time consuming and lacks computational robustness. To this end, linear MPCs have received more attention in the PCC controller design.

In Bedelbayev et al. [39], a linear MPC was developed for the absorber column control. The nonlinear first principle model of the absorber was linearized at given operating point and used as the predictive model. The lean solvent flow rate was selected as the manipulated variable to control the CO_2 capture rate. The inlet flue gas flow rate, temperature and CO_2 content were regarded as measured disturbances and used as a feed-forward signal to the MPC. Simulation results show that the linear MPC could attain a smooth capture rate tracking and quick response to the flue gas variation. Arce et al. [13] presented linear MPCs in a two-layer control structure for the independent solvent regeneration system. Steady-state economic optimization was performed in the high layer to provide optimal set-points. Two linear MPCs were developed in the low layer to track the desired re-boiler level, CO_2 capture molar flow and re-boiler pressure set-points. Zhang et al. [35] developed a linear MPC controller to adjust the CO_2 capture rate and re-boiler temperature for the integrated PCC process via MATLAB MPC toolbox. The lean solvent flow rate and re-boiler steam flow rate were selected as manipulated variables, and the flue gas flow rate, CO_2 composition, rich flow solvent flow rate were considered in the model development as disturbances. Different from the ordinary MPC which use a dynamic control objective function, in [18] and [44], the energy consumptions and CO_2 emissions were taken into account in the MPC's objective function. An optimal scheduling sequence was calculated for the PCC plant. In [40,45,17] different multi-variable linear MPCs were devised to regulate the core variables within the PCC process. Their results all indicated that using the MPC can achieve more superior performance for the flexible operation of the PCC system compared with the conventional PI controllers.

Despite the advantages of the MPC, the performance of MPC greatly relies on the quality of the predictive model. For the aforementioned linear MPCs, the predictive models were all developed through linearization of the mathematical model or through identification at a given operating point. Nevertheless, under the growing demand for flexible operation, the PCC system is required to face the varying flue gas and adjust its capture rate over a wide range. Meanwhile, the re-boiler temperature may also change during the unit load demand change. As these key variables deviate from the model design point, the dynamic behavior of the system will change greatly, and the resulting modeling mismatches will reduce the quality of predictive control and, in severe cases, may destabilize the closed-loop control system.

Owning to this difficulty, the existing linear MPCs only demonstrated their performance around the design point. Understanding the dynamic changes of the system and overcoming their impact on the control system is an important issue for the application of linear MPCs over a wide range of flexible operation of the PCC process.

To attain a wide range load change of the PCC process using the mature linear control technologies, in Wu et al. [46], three linear MPCs were preconfigured at 50%, 80% and 95% capture rate points. During operation, these three controllers were combined together based on the current capture rate to obtain the final global control output. Wu et al. [47] analyzed the dynamic behavior variation and nonlinearity distribution of the PCC process. Based on the results, a suitable operating region was selected, in which a simple linear MPC can achieve a satisfactory capture rate change control. However, the dynamic effect of flue gas flow rate on the PCC system and its variation under different operating conditions has not been analyzed. Moreover, how to effectively overcome the influence of dynamic variations or unknown disturbances was not studied in these works.

Given these observation, the first objective of this paper is to give new insight to the changes of PCC system dynamics under the variation of some key variables, such as flue gas flow rate, CO_2 capture rate and re-boiler temperature. Step response tests under different operating conditions are carried out to observe the changes of dynamics intuitively, and the corresponding response time constants and steady state gains are then analyzed. This investigation will provide useful guidance on the controller design, indicating how to avoid strong changes of PCC process dynamics during the control and provide possible applicable range of the linear MPC.

Then based on the investigation results, a disturbance rejection predictive controller (DRPC) is proposed for the flexible operation of the PCC process. A quasi-infinite horizon function is used as the objective function to improve the performance of conventional MPC and guarantee the stability of the closed-loop system. To overcome the dynamic behavior variations due to changes in operating point and the unknown disturbances due to equipment wear, a disturbance observer is devised to estimate and compensate for their impact on the set-point tracking. In order to enable the predictive controller to promptly adapt to the flue gas flow rate variation, the flue gas flow rate is considered as an additional input in the model development. Thus in the presence of flue gas flow rate change, correct prediction and control action can be provided on time. The simulation studies on an MEA-based post-combustion CO_2 plant developed on the gCCS platform validate the advantages and effectiveness of the proposed DRPC.

2. Process description

The solvent based post-combustion CO_2 capture system considered in this paper is matched with a small scale coal-fired power plant. 30 wt % MEA solvent, which is most commonly used in PCC process is selected as the CO_2 sorbent. At full load condition, the power plant can generate 0.13 kg/s flue gas (CO_2 concentration: 25.2 wt%) using the designated coal. After going through desulfurization, denitrification, dust removal and cooling processes, the flue gas is fed into the bottom of the packed-bed absorber column and contacts with the lean MEA solvent counter currently. The CO_2 in flue gas is absorbed chemically by the MEA solvent, yielding CO_2-enriched solvent and the exited gas is vented into the atmosphere. Next, the rich solvent is pumped into the stripper column across a lean/rich heat exchanger, where it is heated by the steam drawn-off from the intermediate/low-pressure turbine crossover of power plant to release the CO_2. The resulting lean solvent is then resent to the absorber and starts the next cycle. During heating, part of the water and MEA vapor is mixed with the removed CO_2, thus a condenser is used to recollect the fugitive steam and MEA, the separated high purity CO_2 is then compressed and transported to storage.

The dynamic model of this PCC process is established using gCCS toolkit [27,28], which can provide high-fidelity simulation for the CO2 capture, transportation and storage. The specification and parameter selection for the major devices are based on the model developed in [12], which has been verified through field data. The process topology and nominal operation condition of the PCC model are displayed in Fig. 1 and Table 1.

Within the PCC system, there are two variables that are of most concern in the controller design, the CO_2 capture rate and the re-boiler temperature. The CO_2 capture rate is defined as:

$$CO_2\,\text{Capture Rate} = \frac{CO_2\,\textit{in the flue gas} - CO_2\,\textit{in the clean gas}}{CO_2\,\textit{in the flue gas}}, \tag{1}$$

which reflects how well the capture plant completes the carbon reduction task. The re-boiler temperature determines the degree of solvent regeneration, which will affect the ability of lean solvent in CO_2 absorption. On the other hand, an excessively high temperature should be strictly avoided, because it will cause a severe MEA solvent degradation. Considering these issues, these two variables are selected as controlled variables in this study. The lean solvent and re-boiler steam flow rates are selected as the manipulated variables [12,15,16,33–37,41–43,46].

The flexible operation requires the PCC plant to change its capture rate rapidly and follow the flue gas flow rate variation in a wide range. During the dynamic adjustment, the quick change of lean solvent and re-boiler steam flow rates may also cause significant variation of the re-boiler temperature. The change in operating condition of these key variables will cause the process dynamics change and bring in strong impact on the control system. Therefore, this paper investigates the dynamic behavior change of the PCC system under the variation of CO_2 capture rate, flue gas flow rate and re-boiler temperature, providing guidance for the flexible operation of the PCC process and controller development. A disturbance rejection predictive controller is then designed to track the desired CO_2 capture rate in a wide range and maintain the re-boiler temperature at optimal point.

Table 1
Nominal Operating Condition of Some Variables for the PCC Model Developed in gCCS.

Variable	Unit	Value
Flue gas flow rate	[kg/s]	0.13
Flue gas CO_2 concentration	[wt%]	25.2
Flue gas absorber inlet temperature	[K]	313.15
Solvent flow rate	[kg/s]	0.5023
Lean solvent absorber inlet temperature	[K]	313.15
MEA concentration	[wt%]	30
Re-boiler pressure	[bar]	1.79
Re-boiler temperature	[K]	386
Re-boiler liquid level	[m]	0.25
Re-boiler steam flow rate	[kg/s]	0.0366
Condenser Pressure	[bar]	1.69
Condenser temperature	[K]	313.15
Absorber sump liquid level	[m]	1.25
Stripper sump liquid level	[m]	1.25
CO_2 capture rate	[%]	70

Besides the CO_2 capture rate and re-boiler temperature, there are many other variables need to be maintained to guarantee a safe operation of the PCC process. These variables are not strongly coupled or are easily controlled, therefore, PI controllers are designed to maintain them at given levels, which are shown in Fig. 1. Developing a centralized MPC control involving so many variables is a challenging task. Accurate predictive model is difficult to be identified and the receding-horizon calculation of the optimal control sequence is time consuming. Moreover, it is difficult to determine the sampling time of the centralized MPC, because the responses of the variables may be on different time scales.

3. Investigation of the dynamic behavior variation for the PCC process

In this section, step response tests under different working conditions are performed to give an intuitive analysis for the dynamic behavior variation of the solvent-based post-combustion CO_2 capture process. Different from the conventional 2×2 system analysis that only considers the dynamics between MVs (lean solvent and steam flow

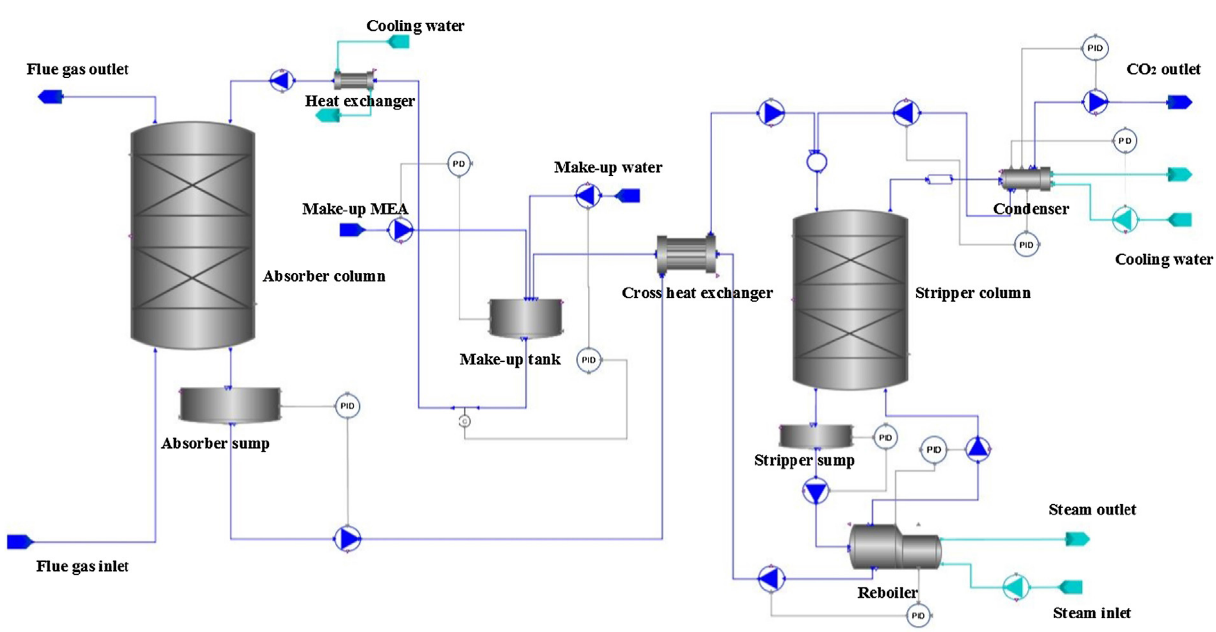

Fig. 1. Schematic diagram of solvent-based PCC process developed on the gCCS platform.

rates) and CVs (capture rate and re-boiler temperature), the influence of main disturbance: the flue gas flue flow rate has also been studied. Three groups of step response tests are conducted to analyze the dynamic behavior of PCC process under: i) different CO_2 capture rates; ii) different flue gas flow rates; and iii) different re-boiler temperatures.

In all the step response tests, the CO_2 capture rate and re-boiler temperature controllers are placed in an open-loop state, while other variables are kept controlled to ensure a normal operating of the CO_2 capture process. Step signals in magnitude of +5% of the respective steady-state values are added to the lean solvent, re-boiler steam and flue gas flow rate channels respectively at different operating points. The relative variation of capture rate and re-boiler temperature based on their initial steady-state values are then calculated and shown in Figs. 2–4.

3.1. CO_2 capture rate change

To investigate the dynamic behavior variation of the PCC process under different CO_2 capture rates, step response tests are carried out at 50%, 60%, 70%, 80%, 90% and 95% capture rates. For all simulation tests in this group, the flue gas flow rate is maintained at 0.13 kg/s and the re-boiler temperature is set as 386 K initially to avoid their influence.

At $t = 1000$ s, step signals in magnitude of +5% of the steady-state values are added to the lean solvent flow rate, re-boiler steam flow rate and flue gas flow rate channels respectively at different CO_2 capture rates. The left column of Fig. 2 shows the step responses of the PCC system corresponding to the step inputs of lean solvent flow rate. At the beginning of the step test, since more lean solvent is fed into the absorber column, more CO_2 in the flue gas can be absorbed, resulting in a prompt rise of CO_2 capture rate. However, as the re-boiler steam flow rate remains at the same level while the rich solvent enters the re-boiler is increased, the re-boiler temperature gradually drops. As a result, less CO_2 can be removed from the solvent and the loading of the lean solvent fed back to the absorber will rise. Therefore, the CO_2 capture rate will drop back to the previous level after a while and its response speed is slower than that of the re-boiler temperature. It takes more than 10,000 s for the PCC process to enter the new steady state, which fully illustrates the system's characteristics of large inertia. However, at the beginning of the step, the rapid impact of lean solvent flow rate on the CO_2 capture rate provides a useful way to achieve a flexible operation of the PCC system, even though it is temporary. On the other hand, the non-minimum phase behavior of the lean solvent flow rate-CO_2 capture rate loop will also bring in difficulties for the conventional feedback controller design.

The dynamic behavior change of the capture system under different capture rates can also be viewed in this column. Regarding the CO_2 capture rate channel, the overall trends of the responses are similar. However, as the capture rate increases, it becomes more difficult to capture the remaining CO_2 in the flue gas, the peak value of the step response drops, especially within 90%-95% capture rate region. On the other hand, the steady-state gains of the step responses slightly decrease and the response speed rises as the capture rate increases. Regarding the re-boiler temperature channel, the dynamic variation of the process is not strong, mainly reflected in the response speed, which has a slight increase as the capture rates rises.

The middle column of Fig. 2 shows the responses of the PCC process at different CO_2 capture rates corresponding to 5% steam flow rate step. The increase of re-boiler steam flow rate will increase the re-boiler temperature directly, as a result, more CO_2 will be released from the rich solvent. The decrease of CO_2 loading will then enhance the CO_2 absorption ability of the lean solvent, thus the CO_2 capture rate will be increased eventually. The response of re-boiler temperature is faster than the response of CO_2 capture rate, but overall very slow. The whole dynamic process will last for more than 10000 s until the capture rate and re-boiler temperature enter the new steady-state. This slow

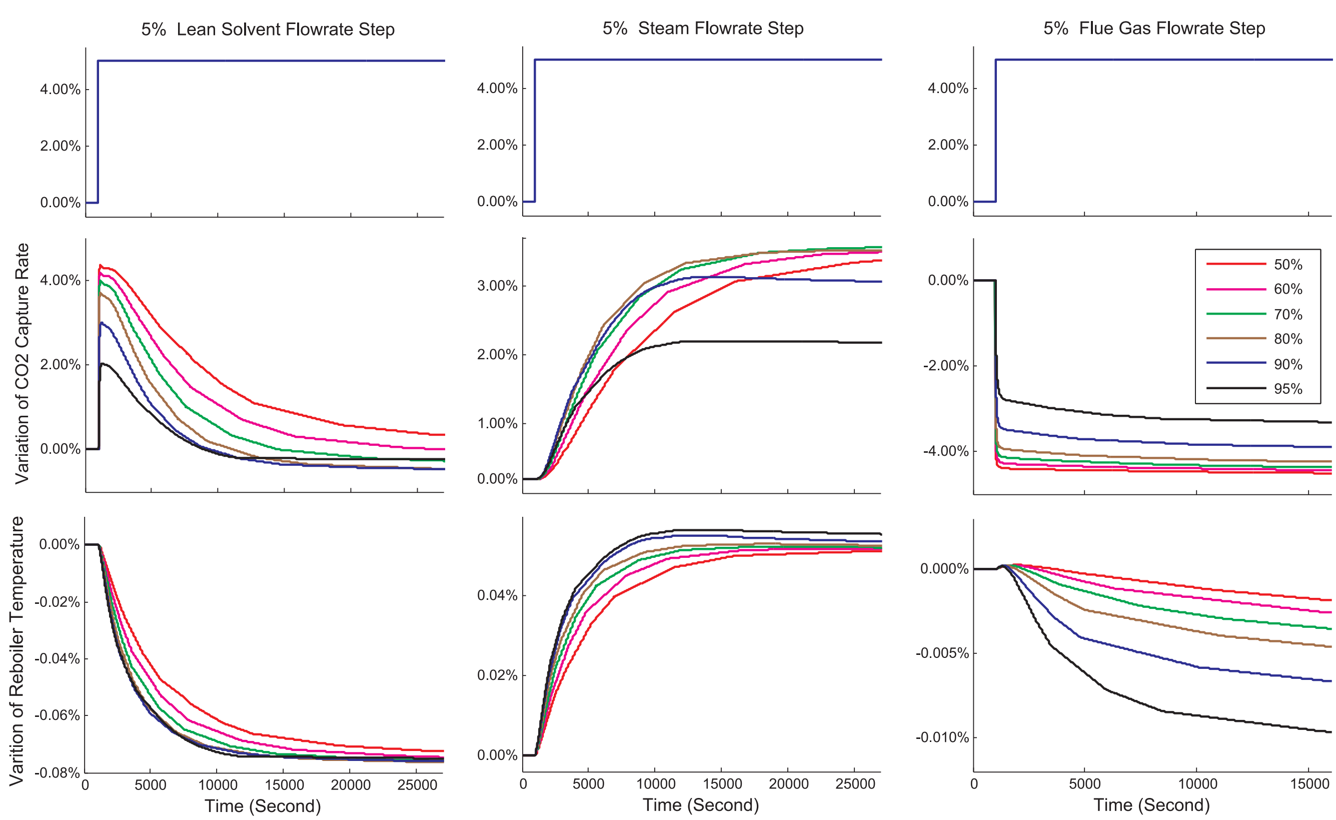

Fig. 2. Responses of the PCC process at six different CO_2 capture rates corresponding to 5% lean solvent flow rate step input (left column), 5% steam flow rate step input (middle column) and 5% flue gas flow rate step input (right column).

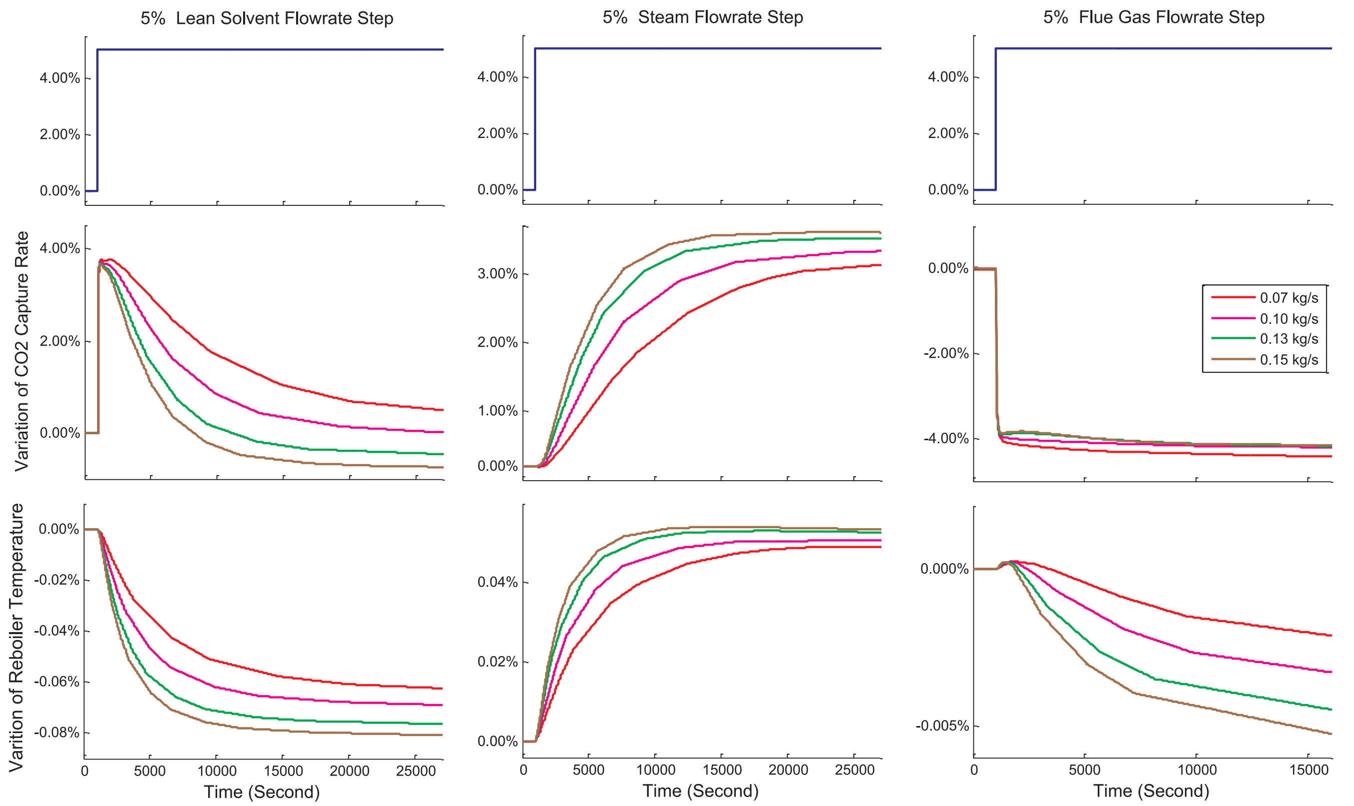

Fig. 3. Responses of the PCC process at four different flue gas flow rates corresponding to 5% lean solvent flow rate step input (left column), 5% steam flow rate step input (middle column) and 5% flue gas flow rate step input (right column).

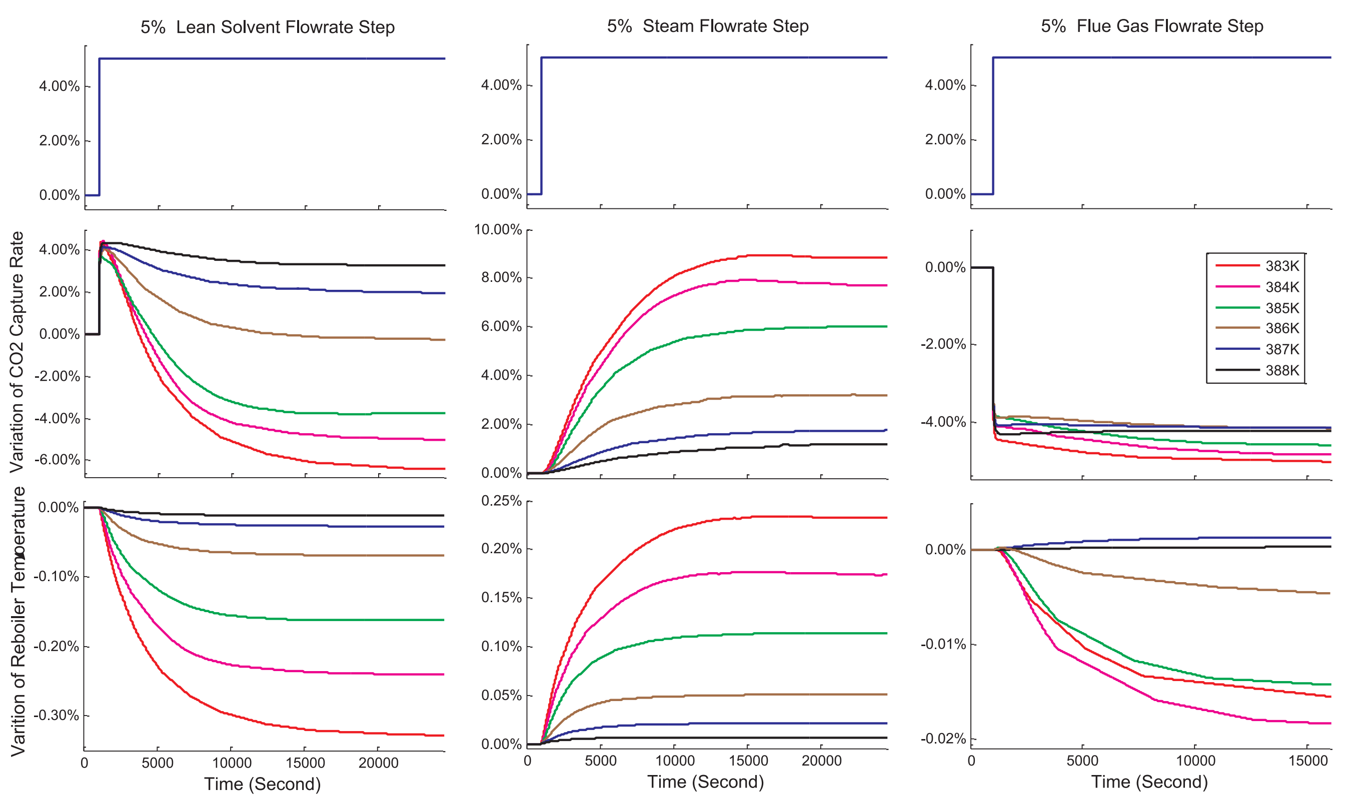

Fig. 4. Responses of the PCC process at six different re-boiler temperature corresponding to lean solvent flow rate step input.

dynamic brings challenges for the flexible operation of the PCC system.

The dynamic behavior change of the capture system under different capture rates is illustrated clearly in this column. Regarding the CO_2 capture rate channel, in the range of 50% to 80%, as the capture rate increases, the steady-state gains of the step responses are similar but the response speed slightly increases. When the capture rate rises to 90%, as most of the CO_2 in the flue gas has been gradually captured, the difficulty for the solvent to absorb the remaining CO_2 begins to increase. As a result, the steady state gain at 90% capture rate has dropped compared with the conditions of lower capture rates. Similarly, when the capture rate rises to 95%, it becomes much difficult to absorb the remaining CO_2 from the flue gas. A huge decrease in steady state gain can thus be found from the middle figure of this column. In terms of the re-boiler temperature, in the range of 50% to 95%, the steady-state gains of the step responses are similar and the response speed slightly increases as the capture rate increases.

We than show the responses of the PCC process corresponding to 5% flue gas flow rate step in the right column of Fig. 2. Because the lean solvent and steam flow rates within the PCC process are not changed, when the inlet flue gas flow rate increases, only a small part of the increased CO_2 can be captured in the absorber. Therefore, according to the calculation formula of capture rate (1), a significant decrease of CO_2 capture rate can be viewed within 100 s of the step test. On the other hand, since more CO_2 is absorbed, the rich solvent loading is increased, which will slightly decrease the re-boiler temperature and then continue decrease the CO_2 capture rate. However, these influence is very limited and can thus be ignored.

It can also be found that under different capture rates, the decrease level of capture rate is different: at high capture rate, capture the CO_2 in the increased flue gas is much easier than capture the remaining CO_2 in the original flue gas. Thus, under 95% and 90% capture rates, there are only 3.3% and 3.9% of capture rates drop corresponding to a 5% flue gas flow rate increase, while around 4.3% of the capture rate drops have occurred under other cases.

The step response tests show that, within 50%-90% capture rate range, the dynamics of the PCC system are similar, nevertheless, its dynamic behavior at 95% capture rate is much different, which is prominently reflected in the re-boiler steam- capture rate channel. Some typical features of the lean solvent flow rate and re-boiler steam flow rate step responses are shown in Tables 2 and 3. For the flue gas flow rate step, since its dynamic response is relatively simple, the main parameters are not listed in the table.

3.2. Flue gas flow rate change

To investigate the dynamic behavior variation of the PCC process under different flue gas flow rates, step response tests are carried out under 0.07 kg/s, 0.10 kg/s, 0.13 kg/s and 0.15 kg/s flue gas flow rates. For all simulation tests in this group, the CO_2 capture rate and the re-boiler temperature are set at 80%, 386 K point initially to avoid their influence. The step responses of the PCC system corresponding to the lean solvent flow rate, re-boiler steam flow rate and flue gas flow rate step inputs are shown in Fig. 3.

Table 3
Typical features for the responses of the PCC process at different CO_2 capture rates corresponding to 5% steam flow rate step input.

CO_2 Capture Rate	Response of CO_2 Capture Rate			Response of Re-boiler Temperature		
	Steady State Gain	Maximum Speed Time	Transient Time	Steady State Gain	Maximum Speed Time	Transient Time
50%	3.178%	3600 s	21113 s	0.051%	1680 s	13673 s
60%	3.294%	3140 s	17349 s	0.052%	1620 s	10824 s
70%	3.358%	2640 s	15700 s	0.052%	1560 s	9514 s
80%	3.317%	2580 s	11821 s	0.053%	1440 s	7565 s
90%	2.864%	2160 s	9346 s	0.054%	1440 s	7218 s
95%	1.982%	2400 s	9233 s	0.056%	1440 s	7565 s

As shown in Fig. 3, there are also some differences for the PCC system dynamics under different flue gas flow rates. Regarding the lean solvent flow rate step (left column), for both the capture rate and re-boiler temperature channels, as the flue gas flow rate rises, the steady-state gain of the step response decreases and the rate of the response increases. Similarly, in case of re-boiler steam flow rate step (middle column), for both the capture rate and re-boiler temperature channels, the steady-state gain and rate of the response increase as the flue gas flow rate rises. However, these dynamic variations are quite limited. There are no major differences for the main trends of the step responses under different flue gas flow rates. In addition, the investigation results also reflect that the PCC system is easily controlled at higher loads, because the manipulated variables can regulate the controlled variables more quickly. For the flue gas flow rate step (right column), the dynamic variation of the PCC system under different flue gas flow rate is very small and can be ignored. Some typical features of the lean solvent flow rate and re-boiler steam flow rate step responses are shown in Tables 4 and 5.

3.3. Re-boiler temperature change

To investigate the dynamic behavior variation of the PCC process under different re-boiler temperatures, step response tests are carried out under 383 K, 384 K, 385 K, 386 K, 387 K and 388 K re-boiler temperatures. For all simulation tests in this group, the flue gas flow rate is maintained at 0.13 kg/s and the CO_2 capture rate is set as 80% initially to avoid their influence. The step responses of the PCC system corresponding to the lean solvent flow rate step input are shown in Fig. 4. It can be seen clearly that, under different re-boiler temperatures, the steady state gains, response speeds and even the variation trends of the step responses are quite different.

In the low temperature range of 383 K to 385 K, the re-boiler heat duty is relatively insufficient, part of the CO_2 cannot be stripped from the rich solvent. Under this condition, the increase of lean solvent flow

Table 2
Typical features for the responses of the PCC process at different CO_2 capture rates corresponding to 5% lean solvent flow rate step input.

CO_2 Capture Rate	Response of CO_2 Capture Rate			Response of Re-boiler Temperature		
	Steady State Gain	Peak Time	Transient Time	Steady State Gain	Maximum Speed Time*	Transient Time*
50%	0.305%	1169 s	19800 s	−0.073%	1680 s	15962 s
60%	0.003%	1173 s	17898 s	−0.075%	1680 s	13592 s
70%	−0.265%	1195 s	15268 s	−0.076%	1620 s	11878 s
80%	−0.362%	1197 s	13633 s	−0.071%	1560 s	10754 s
90%	−0.459%	1234 s	12267 s	−0.076%	1380 s	9868 s
95%	−0.226%	1330 s	9104 s	−0.075%	1380 s	8075 s

*Maximum speed refers to the maximum average rate of change within 60 s of the step response.
Transient time refers to the time it takes for the step response curve to enter the last 5% of the total change (and no longer goes out).

Table 4
Typical features for the responses of the PCC process at different flue gas flow rates corresponding to 5% lean solvent flow rate step input.

Flue Gas Flow Rate	Response of CO_2 Capture Rate			Response of Re-boiler Temperature		
	Steady State Gain	Peak Time	Transient Time	Steady State Gain	Maximum Speed Time	Transient Time
0.07 kg/s	0.471%	2003 s	21106 s	−0.063%	1860 s	16786 s
0.10 kg/s	0.009%	1202 s	17252 s	−0.069%	1620 s	12683 s
0.13 kg/s	−0.362%	1197 s	13633 s	−0.071%	1560 s	10754 s
0.15 kg/s	−0.745%	1184 s	12,270	−0.081%	1500 s	9467 s

rate (left column) will make the re-boiler temperature drop more and increase the CO_2 loading of the lean solvent. As a result, the CO_2 capture rate will decline to a lower level eventually. In the high temperature range of 387 K to 388 K, surplus of re-boiler heat duty has occurred. In this case, the increase of lean solvent flow rate will only cause a slight drop of the re-boiler temperature and increase the CO_2 loading of the lean solvent a little bit. Therefore, the CO_2 capture rate will stay at a higher level eventually. Between these two situations, 386 K is the optimal re-boiler temperature, and under this temperature, the increase of lean solvent flow rate and the resulting increase of lean solvent loading will make the CO_2 capture rate finally go back to the previous level.

As shown in the middle column, under lower re-boiler temperature, the increase of steam flow rate will cause more increase in the capture rate and re-boiler temperature. The reason is that, under lower re-boiler temperature, the heat duty is relatively insufficient, thus the increase of steam flow rate is easier to make the re-boiler temperature rise more, which will achieve a better reduction in lean solvent loading and enhance the CO_2 capture rate. A significant difference of steady-state gains can be viewed within 385 K-387 K region for both the CO_2 capture rate and re-boiler temperature channels.

Similarly, for the flue gas flow rate steps (right column), in case of excess re-boiler heat duty (387 K-388 K), the flue gas flow rate increase has little effect on the re-boiler temperature. However, when the re-boiler heat duty is insufficient (383 K-386 K), the flue gas flow rate increase will make the re-boiler temperature drop more and further cause more drops in CO_2 capture rate.

The investigation results show that the dynamic behavior of the PCC systems changes significantly as the re-boiler temperature change, especially around 386 K, which is the optimal re-boiler temperature for the system operation. This finding also reminds us, it is of great importance to maintain the re-boiler temperature closely around the given optimal set-point, so that the adverse effects of strong dynamic behavior variation on the operation control of PCC process can be alleviated.

Some typical features of the lean solvent flow rate and re-boiler steam flow rate step responses are shown in Tables 6 and 7.

According to the investigation results, the following conclusions can be made for the PCC system dynamics:

(1) In general, the dynamic response of PCC system is very slow, for both the lean solvent and re-boiler steam flow rate steps, more than 2 h is needed for the system to reach the new steady-state. Meanwhile, there are strong couplings among multiple manipulated and controlled variables. These features bring in difficulties for achieving the flexible operation of PCC system;
(2) The lean solvent flow rate can change the CO_2 capture rate in 2–3 min at the beginning stage. Although this quick impact is only temporary, it will provide great help for improving the flexibility of the PCC system. This is the reason why good results can be achieved by using the lean solvent flow rate to control the CO_2 capture rate;
(3) The change of flue gas flow rate will influence the capture rate in a very quick manner, its influence on the re-boiler temperature is trivial;
(4) Under higher flue gas flow rate and capture rates (less than 90%) the PCC system responds more quickly and thus is easy to control;
(5) The dynamic behavior variation of PCC system is small for a CO_2 capture rate change within 50–90% range, however, when the capture rate rises to 95%, the dynamic behavior becomes quite different;
(6) The change of flue gas flow rate will not cause too much dynamic variation for the PCC system; and
(7) Regarding the re-boiler temperature change, the dynamic behavior variation of PCC system is limited within 383–385 K and 387–388 K operating regions. However, for a temperature change within 385–387 K, which is the optimal range for the efficient operation of PCC system, the dynamic behavior variation is very strong.

Remark 3.1:. *The* 5% *step change of input variable is considered in this paper to ensure that the dynamic behavior obtained is the behavior of PCC system closely around the initial operating point. If a big step change is added to the input variable, the system will transit to a point far away from the initial point. It thus will not become clear, which point the dynamic response obtained belongs to and the comparison of dynamic characteristics under different working conditions will become difficult to carry out.*

4. Disturbance rejection predictive controller design for the flexible operation of the solvent-based PCC process

The slow dynamics and multi-variable coupling effect of the capture process motivate us to use MPC to enhance the flexible operation ability of the PCC system. However, in the case of wide range load change, the variation of operating conditions will change the dynamic behavior of the PCC system. The resulting modelling mismatches will degrade the performance of the linear predictive control designed for a given operating point or even cause the control system unstable.

The dynamics investigation results in Section 3 show that, under a wide range of operation, the capture system do have very strong dynamic variations. However, if the control system can maintain the re-boiler temperature tightly around 386 K, which is the optimal

Table 5
Typical features for the responses of the PCC process at different flue gas flow rates corresponding to 5% steam flow rate step input.

Flue Gas Flow Rate	Response of CO_2 Capture Rate			Response of Re-boiler Temperature		
	Steady State Gain	Maximum Speed Time	Transient Time	Steady State Gain	Maximum Speed Time	Transient Time
0.07 kg/s	2.928%	4920 s	19047 s	0.049%	1680 s	14255 s
0.10 kg/s	3.131%	2700 s	15602 s	0.051%	1680 s	10223 s
0.13 kg/s	3.317%	2580 s	11821 s	0.053%	1440 s	7515 s
0.15 kg/s	3.404%	2220 s	10149 s	0.053%	1440 s	6097 s

Table 6
Typical features for the responses of the PCC process at different re-boiler temperatures corresponding to 5% lean solvent flow rate step input.

Re-boiler Temperature	Response of CO_2 Capture Rate			Response of Re-boiler Temperature		
	Steady State Gain	Peak Time	Transient Time	Steady State Gain	Maximum Speed Time	Transient Time
383 K	−6.421%	1153 s	12781 s	−0.329%	1440 s	11483 s
384 K	−5.025%	1319 s	11749 s	−0.241%	1440 s	10035 s
385 K	−3.733%	1088 s	9807 s	−0.162%	1560 s	8306 s
386 K	−0.362%	1197 s	13633 s	−0.071%	1560 s	10754 s
387 K	1.973%	1313 s	15470 s	−0.028%	1380 s	12271 s
388 K	3.265%	1633 s	15277 s	−0.012%	1260 s	9570 s

temperature point, the dynamic variation of the PCC system will become much weaker between 50% and 90% CO_2 capture rates. Therefore, without the need for nonlinear controller, it is possible to design a linear predictive controller to achieve a flexible operation of the PCC system within this range.

In order to further enhance the adaptation ability of the MPC to the flue gas flow rate variation and alleviate the effect of dynamic behavior variation and unknown disturbances, a disturbance rejection predictive controller (DRPC) is proposed in this section for the PCC system operation. The DRPC is composed by an extended state observer, a steady state target calculator and a quasi-infinite horizon MPC. The schematic diagram of the proposed DRPC is illustrated in Fig. 5.

4.1. Predictive model considering the flue gas flow rate disturbance

Considering the operating range of 50% to 90% capture rate, a linear model is identified around 70% capture rate, 386 K re-boiler temperature operating point, which is the middle point within this range. To ensure the MPC can be flexibly adapted to the flue gas flow rate change, the flue gas flow rate f, which is a measured variable in power plant is taken into account as an additional input in the modeling step, resulting in the following state space model:

$$\begin{cases} x_{k+1} = Ax_k + Bu_k + Ef_k \\ y_k = Cx_k + Du_k + Ff_k \end{cases}, \tag{2}$$

where $y_k = [y_{1k} \quad y_{2k}]^T$ is the output vector composed by the CO_2 capture rate and re-boiler temperature, $u_k = [u_{1k} \quad u_{2k}]^T$ is the input vector composed by the lean solvent flow rate u_1 and re-boiler steam flow rate u_2, f_k is the flue gas flow rate, x_k is the state vector, which do not have physical meanings; and A, B, C, D, E, F are the system matrices.

Because the flue gas flow rate is regarded as an additional input, model can be rewritten into an augmented form:

$$\begin{cases} x_{k+1} = Ax_k + \widetilde{B}\widetilde{u}_k \\ y_k = Cx_k + \widetilde{D}\widetilde{u}_k \end{cases}, \tag{3}$$

in which $\widetilde{u}_k = [u_k^T \quad f_k^T]^T$ is the augmented input, and $\widetilde{B} = [B \quad E]$, $\widetilde{D} = [D \quad F]$ are the augmented system matrices. Since model is a standard 3-input, 2-output state space model, using the collected dynamic input, output data sequence, conventional identification approach can be directly employed to identify the system matrices.

4.2. Extended state observer design

To improve the disturbance rejection property of the MPC, i.e., to overcome the issues such as plant behavior variation and unknown disturbances, a disturbance term $d_k \in R^2$ is introduced to the state-space model:

$$\begin{cases} x_{k+1} = Ax_k + \widetilde{B}\widetilde{u}_k + Gd_k \\ y_k = Cx_k + \widetilde{D}\widetilde{u}_k \end{cases} \tag{4}$$

where d_k is a lumped disturbance term representing all the effect of plant behavior variation, modeling mismatches or other unknown disturbances. Because the state vector x_k and the disturbance term d_k are immeasurable, an extended state observer (ESO) is designed to estimate their values:

$$\begin{cases} \begin{bmatrix} \hat{x}_{k+1} \\ \hat{d}_{k+1} \end{bmatrix} = \begin{bmatrix} A & G \\ 0 & I \end{bmatrix}\begin{bmatrix} \hat{x}_k \\ \hat{d}_k \end{bmatrix} + \begin{bmatrix} \widetilde{B} \\ 0 \end{bmatrix}\widetilde{u}_k + L[\hat{y}_k - y_k] \\ \hat{y}_k = C\hat{x}_k + \widetilde{D}\widetilde{u}_k \end{cases} \tag{5}$$

where the symbol "^" indicates the estimation. The observer gain L can be calculated by solving the following Linear matrix inequality (LMI):

$$\begin{bmatrix} M_O^T + M_O - X & (M_O A^{ext} + N_O C^{ext})^T \\ M_O A^{ext} + N_O C^{ext} & X \end{bmatrix} > 0, \tag{6}$$

in which M_O and N_O are matrices, X is a symmetric positive definite matrix and the extended matrices $A^{ext} = \begin{bmatrix} A & G \\ 0 & I \end{bmatrix}$, $C^{ext} = [C \quad 0]$. The ESO gain can be determined by: $L = M_O^{-1}N_O$ [48].

4.3. Steady-state target calculator design

After the lumped disturbance signal is estimated, it will be sent to the following steady-state target calculator (SSTC) - to modify the target value and control input, so that the influence of disturbances on control can be eliminated in time [49].

$$\min_{x_k^s, u_k^s} (u_k^s - u_{ref})^T (u_k^s - u_{ref}) \tag{7}$$

$$s.\ t.\ \begin{bmatrix} x_k^s \\ y_{ref} \end{bmatrix} = \begin{bmatrix} A \\ C \end{bmatrix} x_k^s + \begin{bmatrix} \widetilde{B} \\ \widetilde{D} \end{bmatrix}\begin{bmatrix} u_k^s \\ f_k \end{bmatrix} + \begin{bmatrix} G \\ 0 \end{bmatrix}\hat{d}_k \tag{8}$$

Table 7
Typical features for the responses of the PCC process at different re-boiler temperatures corresponding to 5% steam flow rate step input.

Re-boiler Temperature	Response of CO_2 Capture Rate			Response of Re-boiler Temperature		
	Steady State Gain	Maximum Speed Time	Transient Time	Steady State Gain	Maximum Speed Time	Transient Time
383 K	8.838%	2060 s	10359 s	0.232%	1340 s	9171 s
384 K	7.704%	2300 s	9313 s	0.174%	1400 s	7993 s
385 K	6.021%	2480 s	12068 s	1.142%	1520 s	8812 s
386 K	3.317%	2580 s	11821 s	0.053%	1440 s	7515 s
387 K	1.757%	3080 s	14425 s	0.022%	1040 s	8939 s
388 K	1.200%	17300 s	16270 s	0.007%	1040 s	3712 s

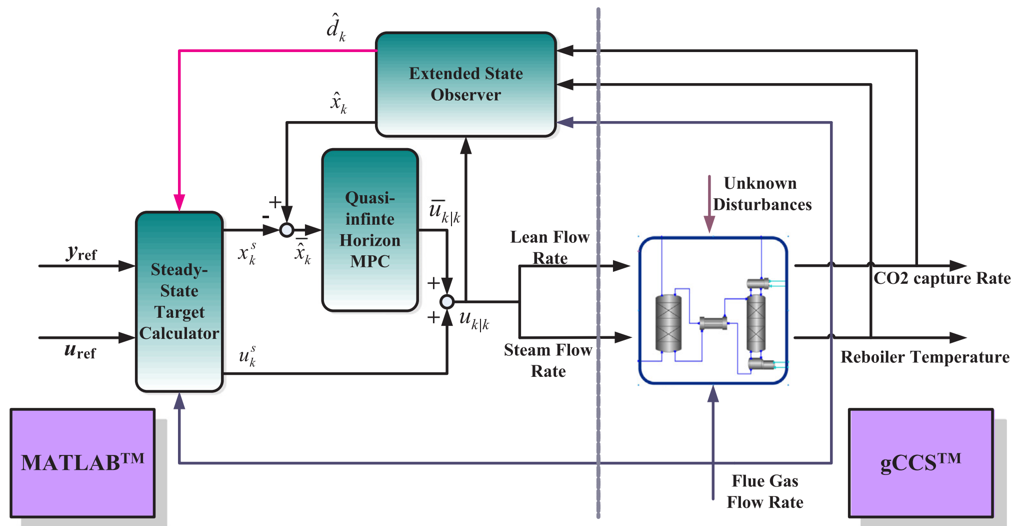

Fig. 5. Schematic diagram of the proposed DRPC for the solvent-based post combustion CO_2 capture system.

$$u_{min} \leqslant u_k^s \leqslant u_{max} \tag{9}$$

Within the SSTC -, y_{ref} and u_{ref} are the desired output set-points and the corresponding input values under nominal condition; u_{min} and u_{max} are the constraints for the input variables. At every sampling time k, by using the static disturbance model (8), the SSTC will adjust the steady state target of the state and input variables x_k^s, u_k^s according to the current flue gas flow rate f_k and the estimated lumped disturbance $\widehat{d}_k$. In this way, the adverse effects of various disturbances can be quickly removed and an offset-free tracking of the desired set-points y_{ref} can be achieved.

Considering the stability of the ESO, subtract from, we can have:

$$\begin{cases} \bar{x}_{k+1} = A\bar{x}_k + B\bar{u}_k \\ \bar{y}_k = C\bar{x}_k + D\bar{u}_k \end{cases}, \tag{10}$$

in which $\bar{x}_k = x_k - x_k^s$, $\bar{u}_k = u_k - u_k^s$, $\bar{y}_k = y_k - y_{ref}$. The system can be used as the predictive model of the MPC, and the goal of the control is to find the optimal constrained control sequence to drive $\bar{y}_k$ to the zero.

4.4. Quasi-infinite horizon MPC design

Considering the control objective function:

$$J_0^{N_p}(k) = \sum_{N=0}^{N_p} [\bar{y}_{k+N|k}^T Q_0 \bar{y}_{k+N|k} + \bar{u}_{k+N|k}^T R_0 \bar{u}_{k+N|k}], \tag{11}$$

where $\bar{y}_{k+N|k}$, (N: $0-N_p$) is the prediction of future output and $\bar{u}_{k+N|k}$, (N: $0-N_p$) is the future control input sequence; Q_0 and R_0 are the weighting matrices for the output and input, respectively. A regular MPCs with enhanced disturbance rejection property can be designed for the PCC process. At every sampling time k, through minimization of subject to corresponding input magnitude and rate constraints, the optimal future control sequence $\bar{u}_{k+N|k}$, (N: $0-N_p$) can be calculated. The first control input $u_{k|k} = \bar{u}_{k|k} + u_k^s$ can be selected as the current control action and implemented on the PCC plant.

Note that the selection of this objective function requires the controller to track the desired CO_2 capture rate set-point rapidly and smoothly while maintaining the re-boiler temperature closely around its optimal value to avoid the huge dynamics change of the system. On the other hand, during the operation, the lean solvent flow rate and re-boiler steam flow rate are expected to be as small as possible, so that better economic performance can be attained.

One issue for applying the regular MPCs on the PCC process is that, a large predictive horizon is usually needed to ensure a satisfactory control quality and system stability, because the PCC process has very slow dynamics. Such a method will increase the computational cost of the controller. To overcome this issue, a quasi-infinite horizon MPC [50] is selected in this section for the PCC system control.

Consider an infinite horizon control objective function

$$J_0^{\infty}(k) = \sum_{N=0}^{\infty} [\bar{y}_{k+N|k}^T Q_0 \bar{y}_{k+N|k} + \bar{u}_{k+N|k}^T R_0 \bar{u}_{k+N|k}] \tag{12}$$

divide the future control sequence $\bar{u}_{k+N|k}$, (N: $0-\infty$) into two part: free control sequence $\bar{U}_k = [\bar{u}_{k|k} \;\; \bar{u}_{k+1|k} \;\; \cdots \;\; \bar{u}_{k+N_f-1|k}]$ like conventional MPC for $0 \leq N < N_f$ and feedback control sequence $\bar{u}_{k+N|k} = YG^{-1}\bar{x}_{k+N|k}$ for $N \geq N_f$, in which Y and G are matrices. By finding γ, the upper bound of the infinite horizon function, and minimizing it, the optimal control sequence can be determined from solving the following LMIs:

$$\min_{\gamma, \bar{U}_k, Y, G, \widetilde{S}} \gamma$$
$$s.\,t.\; (14) - (17) \tag{13}$$

$$\begin{bmatrix} 1 & * & * & * & * \\ l_x\bar{\hat{x}}_k + l_u\bar{U}_k & \frac{\widetilde{S}}{2} & 0 & 0 & 0 \\ Q^{1/2}(L_x\bar{\hat{x}}_k + L_u\bar{U}_k) & 0 & \frac{\gamma I}{2} & 0 & 0 \\ R^{1/2}\bar{U}_k & 0 & 0 & \gamma I & 0 \\ l_x w & 0 & 0 & 0 & \frac{\widetilde{S}}{2} \end{bmatrix} \geqslant 0 \tag{14}$$

$$\begin{bmatrix} G + G^T - \widetilde{S} & * & * & * \\ (AG + BY) & \widetilde{S} & 0 & 0 \\ Q_0^{1/2}(CG + DY) & 0 & \gamma I & 0 \\ R_0^{1/2} Y & 0 & 0 & \gamma I \end{bmatrix} > 0 \tag{15}$$

$$\begin{bmatrix} I_2 \\ I_2 \\ \vdots \\ I_2 \end{bmatrix} (u_{min} - u_k^s) \leqslant \bar{U}_k \leqslant \begin{bmatrix} I_2 \\ I_2 \\ \vdots \\ I_2 \end{bmatrix} (u_{max} - u_k^s) \tag{16}$$

$$\begin{bmatrix} I_2 \\ I_2 \\ \vdots \\ I_2 \end{bmatrix} \Delta u_{min} \leqslant \zeta \left[\bar{U}_k + \begin{bmatrix} u_{k-1} \\ I_2 \\ I_2 \\ \vdots \\ I_2 \end{bmatrix} u_k^s \right] \leqslant \begin{bmatrix} I_2 \\ I_2 \\ \vdots \\ I_2 \end{bmatrix} \Delta u_{\max} \tag{17}$$

where $Q = I_{N_f} \otimes Q_0$, $R = I_{N_f} \otimes R_0$, w is the upper bound of the state

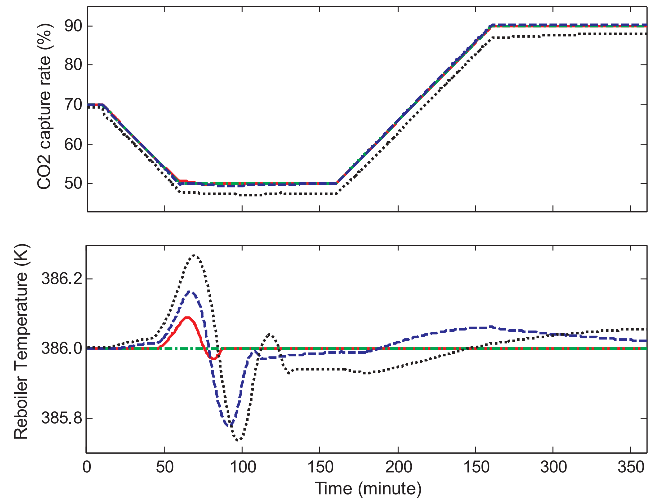

Fig. 6. Performance of the PCC system for a 70%-50%-90% CO_2 capture rate change: output variables (solid in red: DRPC; dashed in blue: MPC_I; dotted in black: MPC; dot-dashed in green: reference). (For interpretation of the references to colour in this figure legend, the reader is referred to the web version of this article.)

estimation error, $\hat{\tilde{x}}_k = \hat{x}_k - x_k^s$ and $\zeta = \begin{bmatrix} -I_2 & I_2 & 0 & \dots & 0 \\ 0 & -I_2 & I_2 & \dots & \vdots \\ \vdots & \vdots & \ddots & \ddots & 0 \\ 0 & \cdots & 0 & -I_2 & I_2 \end{bmatrix}$. The prediction matrices l_x, l_u, l_x, l_u,can be obtained by stacking up the predictive model:

$$l_u = [A^{N_f-1} \quad A^{N_f-2} \quad \dots \quad A^0]B,$$

$$L_x = \begin{bmatrix} C \\ CA \\ \vdots \\ CA^{N_f-1} \end{bmatrix}, \ L_u = \begin{bmatrix} D & 0 & \cdots & 0 \\ CB & D & \cdots & 0 \\ \vdots & \ddots & \cdots & 0 \\ CA^{N_f-2}B & \cdots & CB & D \end{bmatrix}.$$

The LMI guarantees that, γ is the upper bound of the infinite objective function, gives the Lyapunov stability constraint of the closed loop control system, and are the magnitude and rate constraints of the free input variables. At each sampling time, the first element in the solved control sequence $\bar{u}_{k|k}$ is added to the target input u_k^s, the resulting $u_{k|k} = \bar{u}_{k|k} + u_k^s$ is selected as the current control action and implemented on the PCC plant.

The proposed DRPC has the following advantages for the flexible operation of the PCC process:

(1) Flue gas flow rate variation of upstream power plant is a major disturbance to the PCC process. To overcome this issue, the flue gas flow rate is used as an additional input in the model development based on the idea of feed-forward control. Then by using the ESO and SSTC, the proposed DRPC can change the target input u_k^s immediately according to the current flue gas flow rate, thus the control action $u_{k|k} = \bar{u}_{k|k} + u_k^s$ can be promptly adjusted, making the capture system flexibly adapt to the flue gas flow rate change;
(2) Plant dynamic variations due to wide range of operation and other unknown disturbances will bring in many adverse effects to the control of PCC process. For this reason, the ESO and SSTC are designed in the DRPC structure to estimate the disturbances and eliminate their impact, enhance the disturbance rejection property of the MPC; and
(3) A quasi-infinite horizon MPC is applied for the PCC process. By including the infinite future control moves into a feedback control law, only a fewer prediction steps are required to achieve a satisfactory control of the slow PCC process.

Remark 4.1:. *For the initialization of the MPC, we assume that the PCC system is in steady state at the initial moment and there are no lumped disturbances ($\hat{d}_k = 0$). Then according to the current input u_k, output y_k ($y_k = y_{ref}$, $u_k = u_{ref}$) and flue gas flow rate f_k, x_k^scan be calculated by equation (7)-(9), which is set as the initial state$\hat{x}_k$.*

5. Simulation results

This section verifies the control effect of DRPC for the flexible operation of the PCC process under wide range CO_2 capture rate change, flue gas flow rate change and unknown disturbances. Linear state space model identified around 70% capture rate, 386 K operating point for re-boiler temperature is selected as the predictive model, since it is a middle point within the considered operating range (50%-90% capture rates). The parameters of the proposed DRPC are set as follows: sampling time $T_s = 30$ s, free control input number $N_f = 2$, disturbance matrix $G = diag(0.1, 0.08)$, upper bound of the state estimation error $w = [1 \quad 1]^T$. A too small w will limit the feasibility of the DRPC; and a too large w will influence the initial status of the predictive control system. Considering the objectives of the PCC system control:1) quickly track the CO_2 capture rate set-point; 2) maintain the re-boiler temperature at optimal point to avoid plant behavior variation; and 3) reduce the lean solvent and re-boiler steam flow rate as much as possible to lower the energy consumption, the weighting matrices are set as $Q_0 = diag(10, 1)$, $R_0 = diag(1, 1)$. Input magnitude and rate constraints are taken into account: $u_{\min} = [0.2 \quad 0.005]^T$, $u_{\max} = [1 \quad 0.08]^T$, $\Delta u_{\min} = [-0.007 \quad -0.001]^T$, $\Delta u_{\max} = [0.007 \quad 0.001]^T$ due to the physical limitations of the valves and pumps.

Two other MPCs are designed for the purpose of comparison: a) the conventional MPC with integral action (MPC_I); b) conventional MPC without using the integral action (MPC). The predictive model, sampling time and weighting matrices of these two MPCs are set the same as the DRPC. The prediction horizon N_p is set as 6 steps (180 s) because too small N_p is very easy to cause system instability.

The three predictive controllers are developed in MATLAB platform and run with a sample period of 30 s. At each sampling time during the simulation, the controllers and the gCCS plant model communicated with each other through the gO:MATLAB interface.

Case 1: Wide range CO_2 capture rate change is considered in the first simulation since it is a basic requirement for the flexible operation of the PCC process. We suppose that the PCC system is operating at 70% capture rate point initially, then according to the instruction of scheduling level, at $t = 10$ min and $t = 160$ min, the set-point changes to 50% and 90% at the ramping rate of 0.4%/min respectively. During the CO_2 capture rate variation, the set-point of re-boiler temperature controller is fixed at 386 K.

The results in Figs. 6 and 7 indicate that all the three linear predictive controllers can attain a satisfactory control performance for the CO_2 capture rate change within 50%-90% operating region. When the capture rate set-point varies, the predictive controllers adjust the lean solvent and re-boiler steam flow rates coordinately, the CO_2 capture rate can thus follow the changed set-point closely and smoothly. At the same time, the re-boiler temperature can also be kept tightly around the desired point, ensuring an economical running of the PCC process and avoiding the adverse impact of strong dynamic changes on the control system.

By using the ESO and SSTC to estimate and quickly compensate the effect of dynamic variation during the capture rate change, the proposed DRPC has the best performance among the three linear predictive controllers. The deviation of the re-boiler temperature is less than 0.1 K and the steam flow rate fluctuation during the transition of regulation is quite small. Note that with the use of quasi-infinite horizon MPC in the DRPC framework, the free control input number is set quite small as $N_f = 2$, which means that the computational effort for the DRPC could be very small. With the integral action being included in the MPC design, an offset free tracking performance can also be achieved by the

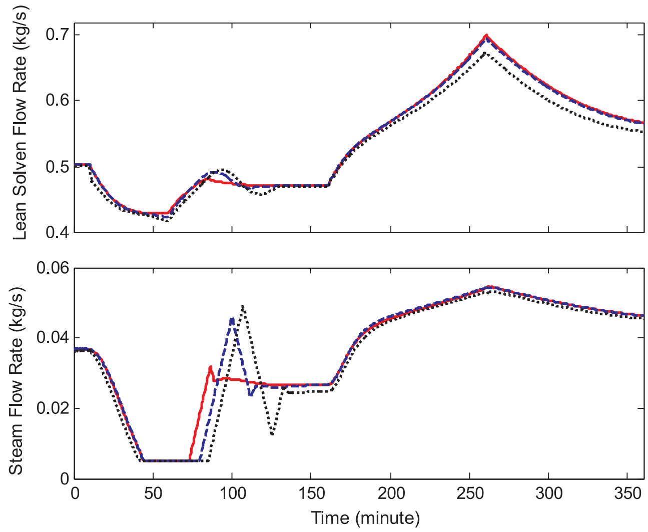

Fig. 7. Performance of the PCC system for a 70%-50%-90% CO_2 capture rate change: manipulated variables (solid in red: DRPC; dashed in blue: MPC_I; dotted in black: MPC). (For interpretation of the references to colour in this figure legend, the reader is referred to the web version of this article.)

MPC_I, however, in the case of small predictive horizon, the performance of MPC_I is worse than the DRPC, which is mainly reflected in the re-boiler temperature control. For the conventional MPC, since no means are used to compensate for the effects of dynamic change, it has the worst performance. Control offset is occurred for both the CO_2 capture rate and re-boiler temperature.

Case 2: Flue gas flow rate change is then considered in the second simulation to test the performance of the linear MPCs. We assume that at $t = 10$ min and $t = 125$ min, due to the power load variation of upstream power plant, the flue gas flow rate changes from 0.13 kg/s to 0.07 kg/s and 0.15 kg/s respectively. During the simulation, the set-points for CO_2 capture rate and re-boiler temperature are fixed at 70% and 386 K. The results are illustrated in Figs. 8 and 9.

The simulation results demonstrate that the proposed DRPC can effectively handle the variation of flue gas flow rate. As shown in Figs. 2–4, the dramatic change of the flue gas flow rate will cause large changes in CO_2 capture rate rapidly and make it deviate far away from the desired set-point under open loop situation. However, because the flue gas flow rate f has already been considered in the predictive model development, through the calculation of SSTC, the DRPC can regulate the lean solvent and re-boiler steam flow rate in time, according to the current flue gas flow rate. As a result, it can be seen in Fig. 8 that, the capture rate can be quickly controlled back to the set-point and the fluctuation of re-boiler temperature during the regulation is greatly reduced.

For the other two MPCs, their performance is much worse than the proposed DRPC. In the presence of flue gas flow rate variation, their prediction and control performance is greatly degraded since the flue gas is not considered in the model development. Regarding the conventional MPC, large control offset is occurred for the CO_2 capture rate, and the re-boiler temperature has continued to swing around the given set-point. Meanwhile, the lean solvent and steam flow rates also exhibit a greater degree of oscillation compared with the performance of DRPC. Regarding the MPC_I, the use of integral action reduces the stability of the control system. Severe fluctuation can be viewed for both the capture rate and re-boiler temperature in Fig. 8 and for steam flow rate in Fig. 9. The PCC system is not able to run smoothly under the strong variation of flue gas flow rate.

Case 3: We then devise the last simulation to test the performance of the linear predictive controllers in the presence of unknown disturbances. Similarly, we suppose that the PCC plant is operating at 70% capture rate operating point initially, due to some unknown equipment failures, at $t = 50$ min, the lean solvent flow rate is reduced by 0.1 kg/s, then at $t = 150$ min, the re-boiler steam flow rate is increased by 0.0074 kg/s. The set-points for CO_2 capture rate and re-boiler temperature are fixed at 70% and 386 K during the simulation.

The simulation results shown in Figs. 10 and 11 illustrate the effectiveness of the proposed DRPC in handling the impact of unknown disturbances. At $t = 50$ min, the unknown decrease of lean solvent flow rate makes the CO_2 capture rate and re-boiler temperature increase rapidly. The DRPC estimates the value of disturbance $\hat{d}_k$ from the control action and actual plant output via the ESO, then quickly modifies the lean solvent and steam flow rates according to the value of $\hat{d}_k$ through the SSTC. Following this, the impact of unknown disturbances can be rapidly rejected by the DRPC system. The same situation also occurs at $t = 150$ min, when unknown increase of steam flow rate make the CO_2 capture rate and re-boiler temperature rise. The DRPC can drive them back to the set-points with minimal fluctuations and time. On the other hand, by including the integral action, the MPC_I can also alleviate the influence of unknown disturbances, however, its performance is worse than the DRPC, stronger fluctuation can be viewed from the re-boiler temperature control. For the conventional MPC, the influence of unknown disturbances cannot be eliminated, large control offset is thus occurred, especially for the CO_2 capture rate.

The three simulations demonstrate the advantages of the proposed DRPC in the operation of the PCC process. The DRPC can quickly change the CO_2 capture rate in a wide range, respond flexibly to the flue gas flow rate variation and effectively overcome the impact of unknown disturbances.

6. Conclusion

This paper investigated the dynamic behavior and its variation of the PCC system to provide guidance for the controller design. The variation of three key variables during the PCC flexible operation are

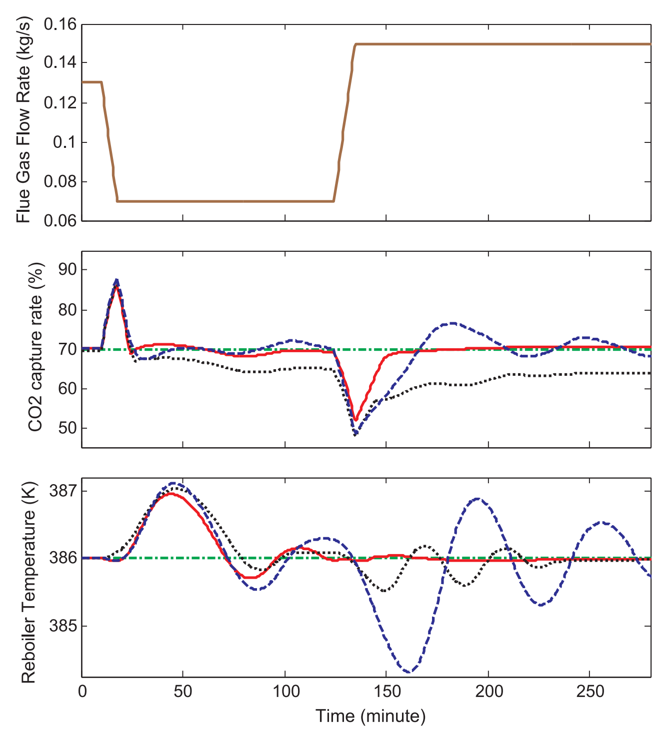

Fig. 8. Performance of the PCC system in the presence of power plant flue gas variation: output variables (solid in red: DRPC; dashed in blue: MPC_I; dotted in black: MPC; dot-dashed in green: reference). (For interpretation of the references to colour in this figure legend, the reader is referred to the web version of this article.)

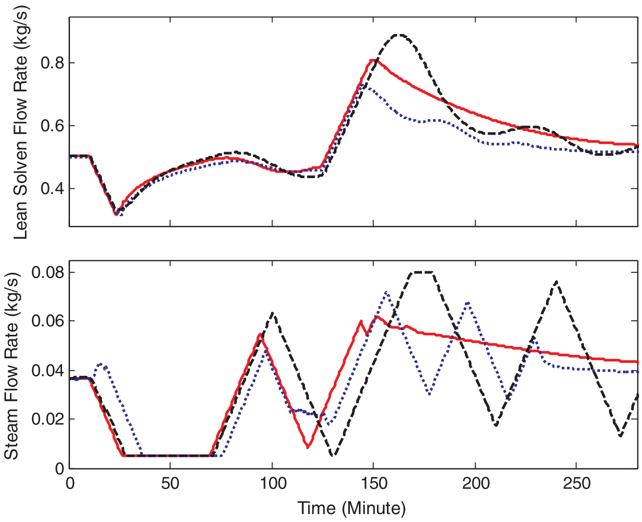

Fig. 9. Performance of the PCC system in the presence of power plant flue gas variation: manipulated variables (solid in red: DRPC; dashed in blue: MPC_I; dotted in black: MPC). (For interpretation of the references to colour in this figure legend, the reader is referred to the web version of this article.)

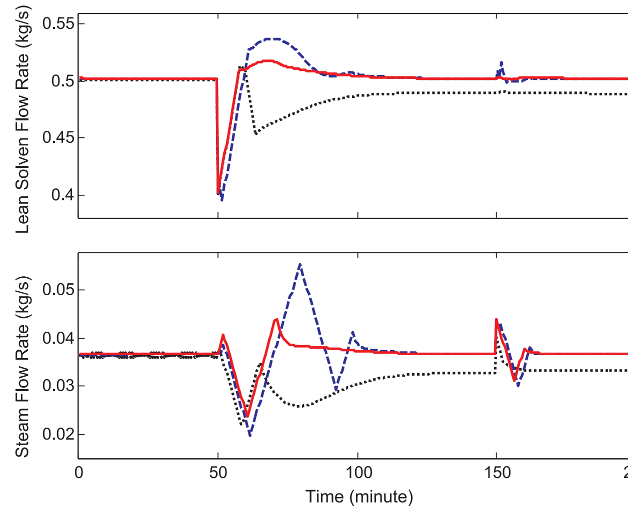

Fig. 11. Performance of the PCC system in the presence of unknown disturbances: manipulated variables (solid in red: DRPC; dashed in blue: MPC_I; dotted in black: MPC). (For interpretation of the references to colour in this figure legend, the reader is referred to the web version of this article.)

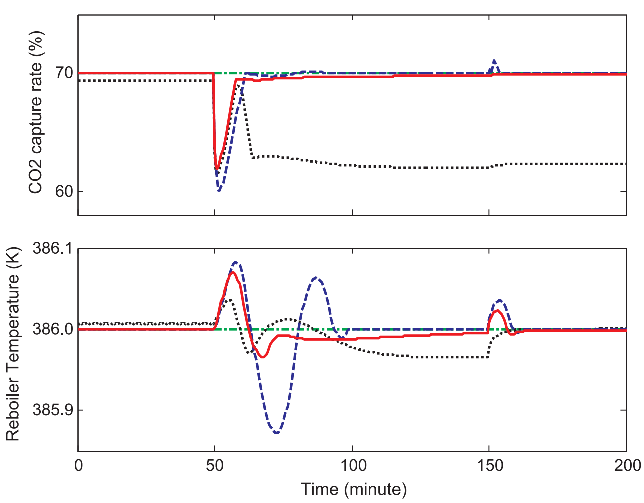

Fig. 10. Performance of the PCC system in the presence of unknown disturbances: output variables (solid in red: DRPC; dashed in blue: MPC_I; dotted in black: MPC; dot-dashed in green: reference). (For interpretation of the references to colour in this figure legend, the reader is referred to the web version of this article.)

taken into account: the CO_2 capture rate, the power plant flue gas flow rate and the re-boiler temperature. Step response tests at different operating points are performed to display the dynamic characteristics of the PCC system intuitively.

The investigation results fully illustrate the slow dynamics of the PCC system and the strong couplings among the key variables. The dynamic behavior variation of the PCC system is also exhibited, that: 1) under higher capture rate and flue gas flow rate, the responses of PCC system is quicker compared with lower conditions 2) there are two regions within which the dynamic variation of the PCC system is quite strong: around 90%-95% capture rate range and around 386 K, the optimal re-boiler temperature point.

To overcome the control difficulties of the PCC system and enhance the performance of conventional MPC in the presence of dynamic variations, a disturbance rejection predictive controller (DRPC) is developed for the PCC process. By considering the effects of flue gas flow rate in the predictive model development and coordinated using the extended state observer (ESO), steady state target calculator (SSTC) and a quasi-infinite horizon MPC. The DRPC can quickly adapt to the flue gas flow rate change, eliminate the effect of plant behavior variation and unknown disturbances and achieve a wide range of capture rate change using very small prediction steps. Simulation results on an MEA based PCC plant verify the advantages and effectiveness of the proposed DRPC.

Acknowledgements

The authors would like to acknowledge the National Natural Science Foundation of China (NSFC) under Grant 51506029, the Natural Science Foundation of Jiangsu Province, China under Grant BK20150631, China Postdoctoral Science Foundation, Jiangsu Province Postdoctoral Science Foundation, EU FP7 International Staff Research Exchange Scheme on power plant and carbon capture (Ref: PIRSES-GA-2013-612230) and the Royal Society- Sino British Fellowship Trust International Fellowship for funding this work.

References

[1] IPCC. Special report on carbon dioxide capture and storage. Cambridge, UK: Cambridge University Press; 2005.
[2] IPCC. Climate change 2007: synthesis report. Contribution of working groups I, II and III to the fourth assessment report of the intergovernmental panel on climate change (pp. 30–37). Geneva, Switzerland, 2007.
[3] IEA. Energy Technology Perspectives 2008. IEA/OECD, Paris, France, 2008.
[4] Oexmann J. Post-Combustion CO_2 Capture: Energetic Evaluation of chemical Absorption Processes in Coal-Fired Steam Power Plants. Ph.D. thesis, Technische Universitat Hamburg-Harburg 2011.
[5] Oexmann J, Hensel C, Kather A. Post-combustion CO_2-capture from coal-fired power plants: preliminary evaluation of an integrated chemical absorption process with piperazine-promoted potassium carbonate. Int J Greenhouse Gas Control 2008;2:539–52.
[6] Mores P, Rodríguez N, Scenna N, Mussati S. CO_2 capture in power plants: Minimization of the investment and operating cost of the post-combustion process using MEA aqueous solution. Int J Greenhouse Gas Control 2012;10:148–63.
[7] Raksajati A, Ho MT, Wiley DE. Reducing the cost of CO_2 capture from flue gases using aqueous chemical absorption. Ind Eng Chem Res Nov 2013;52(47):16887–901.
[8] Karimi M, Svendsen HF, Hillestad M. Capital costs and energy considerations of different alternative stripper configurations for post combustion CO2 capture. Chem Eng Res Des 2011;89(8):1229–36.
[9] Duan L, Zhao M, Yang Y. Integration and optimization study on the coal-fired power plant with CO2 capture using MEA. Energy 2012;45:107–16.
[10] Chen Q, Kang C, Xia Q, Kirschen DS. Optimal flexible operation of a CO_2 capture power plant in a combined energy and carbon emission market. IEEE Trans Power Syst Aug. 2012;27(3):1602–8.
[11] Lawal A, Wang M, Stephenson P, Obi O. Demonstrating full-scale post-combustion CO_2 capture for coal-fired power plants through dynamic modelling and simulation.

Fuel 2012;101:115–28.
[12] Lawal A, Wang M, Stephenson P, Koumpouras G, Yeung H. Dynamic modelling and analysis of post-combustion CO_2 chemical absorption process for coal-fired power plants. Fuel 2010;89:2791–801.
[13] Arce A, Mac Dowell N, Shah N, Vega LF. Flexible operation of solvent regeneration systems for CO_2 capture processes using advanced control techniques: towards operational cost minimization. Int J Greenhouse Gas Control 2012;11:236–50.
[14] Manaf NA, Qadir A, Abbas A. The hybrid MPC-MINLP algorithm for optimal operation of coal-fired power plants with solvent based post-combustion CO_2 capture. Petroleum 2017;3:155–66.
[15] Lin Y, Pan T, Wong D, Jang S, Chi Y, Yeh C. Plantwide control of CO_2 capture by absorption and stripping using monoethanolamine solution. Ind Eng Chem Res 2011;50:1338–45.
[16] Lin Y, Wong D, Jang S. Control strategies for flexible operation of power plant with CO_2 capture plant. AIChE J 2012;58(9):2697–704.
[17] Cormos A, Vasile M, Cristea M. Flexible operation of CO2 capture processes integrated with power plant using advanced control techniques. In: 12th International Symposium on Process Systems Engineering and 25th European Symposium on Computer Aided Process Engineering, Copenhagen, Denmark, May 31-Jun 4, 2015.
[18] He Z, Sahraei MH, Recardez-Sandoval LA. Flexible operation and simultaneous scheduling and control of a CO_2 capture plant using model predictive control. Int J Greenhouse Gas Control 2016;48:300–11.
[19] Bui M, Gunawan I, Verheyen V, Feron P, Meuleman E. Flexible operation of CSIRO's post-combustion CO_2 capture pilot plant at the AGL Loy Yang power station. Int J Greenhouse Gas Control 2016;48:188–203.
[20] Zaman M, Jang H, Rizman M, Lee JH. Optimal design for flexible operation of the post-combustion CO_2 capture plant with uncertain economic factors. Comput Chem Eng 2016;84:199–207.
[21] Wu X, Shen J, Li Y, Lee KY. Steam power plant configuration, design and control. WIREs. Energy Environ 2015;4(6):537–63. Nov-Dec.
[22] Lawal A, Wang M, Stephenson P, Yeung H. Dynamic modelling of CO_2 absorption for post combustion capture in coal-fired power plants. Fuel 2009;88:2455–62.
[23] Ziaii S, Rochelle GT, Edgar TF. Dynamic modeling to minimize energy use for CO_2 capture in power plants by aqueous monoethanolamine. Ind Eng Chem Res 2009;48(13):6105–11.
[24] Dietl K, Joos A, Schmitz G. Dynamic analysis of the absorption/desorption loop of a carbon capture plant using an object-oriented approach. Chem Eng Process Process Intensif 2012;52:132–9.
[25] Montañés RM, Nord LO. Dynamic Simulations of the Post-combustion CO2 Capture System of a Combined Cycle Power Plant. In: 12th International Modelica Conference, Prague, Czech Republic, May 15-17, 2017.
[26] Jayarathna SA, Lie B, Melaaen MC. Amine based CO_2 capture plant: dynamic modeling and simulations. Int J Greenhouse Gas Control 2013;14:282–90.
[27] Rodriguez J, Andrade A, Lawal A, Samsatli N, Calado S, Lafitte T, et al. An integrated framework for the dynamic modelling of solvent-based CO_2 capture processes. Energy Procedia 2014;63:1206–17.
[28] Mechleri E, Lawal A, Ramos A, Davison J, Dowell NM. Process control strategies for flexible operation of post-combustion CO_2 capture plants. Int J Greenhouse Gas Control 2017;57:14–25.
[29] Li F, Zhang J, Oko E, Wang M. Modelling of a post-combustion CO_2 capture process using neural networks. Fuel 2015;151:156–63.
[30] Manaf NA, Cousins A, Feron P, Abbas A. Dynamic modelling. Identification and preliminary control analysis of an amine-based post-combustion CO_2 capture pilot plant. J Cleaner Prod 2016;113:635–53.
[31] Zhou Q, Chan CW, Tontiwachwuthikul P, Idem R, Gelowitz D. Application of neuro-fuzzy technique for operational problem solving in a CO_2 capture process system. J Greenhouse Gas Control 2013;15:32–41.
[32] Faber R, Kopcke M, Biede O, Knudsen JN, Andersen J. Open-loop responses for the MEA post combustion capture process: exprimental results from the Esbjerg pilot plant. Energy Procedia 2011;4:1427–34.
[33] Panahi M, Skogestad S. Economically efficient operation of CO_2 capturing process part I: self-optimizing procedure for selecting the best controlled variables. Chem Eng Process Process Intensif 2011;50(3):247–53.
[34] Panahi M, Skogestad S. Economically efficient operation of CO_2 capturing process part II: Design of control layer. Chem Eng Process Process Intensif 2012;52:112–24.
[35] Zhang Q, Turton R, Bhattacharyya D. Development of model and model-predictive control of an MEA-based post-combustion CO_2 capture process. Ind Eng Chem Res 2016;55:1292–308.
[36] Nittaya T, Douglas PL, Croiset E, Ricardez-Sandoval LA. Dynamic modelling and control of MEA absorption processes for CO_2 capture from power plants. Fuel 2014;116:672–91.
[37] Nittaya T, Douglas PL, Croiset E, Ricardez-Sandoval LA. Dynamic Modeling and Evaluation of an Industrial-Scale CO_2 Capture Plant Using Monoethanolamine Absorption Processes. Ind Eng Chem Res 2014;53:11411–26.
[38] Posch S, Haider M. Dynamic modelling of CO_2 absorption from coal-fired power plants into an aqueous monoethanolamine solution. Chem Eng Res Des 2013;91:977–87.
[39] Bedelbayev A, Greer T, Lie B. Model based control of absorption tower for CO2 capturing. In: 49th Scandinavian Conference on Simulation and Modeling, Oct 2008.
[40] Mehleri ED, Mac Dowell N, Thornhill NF. Model predictive control of post-combustion CO2 capture process integrated with a power plant. In: 12th International Symposium on Process Systems Engineering and 25th European Symposium on Computer Aided Process Engineering, Copenhagen, Denmark, May 31-Jun 4, 2015.
[41] Åkesson J, Laird CD, Lavedan G, Prölß K, Tummescheit H, Velut S, et al. Nonlinear Model Predictive Control of a CO_2 Post-Combustion Absorption Unit. Chem Eng Technol 2012;35(3):445–54.
[42] Prölß K, Tummescheit H, Velut S, Åkesson J. Dynamic model of a post-combustion absorption unit for use in a non-linear model predictive control scheme. Energy Procedia 2011;4:2620–7.
[43] Zhang Q, Turton R, Bhattacharyya D. Nonlinear model predictive control and H_∞ robust control for a post-combustion CO_2 capture process. Int J Greenhouse Gas Control 2018;70:105–16.
[44] Sahraei MH, Ricardez-Sandoval LA. Controllability and optimal scheduling of a CO_2 capture plant using model predictive control. Int J Greenhouse Gas Control 2014;30:58–71.
[45] Luu MT, Manaf NA, Abbas A. Dynamic modelling and control strategies for flexible operation of amine-based post-combustion CO_2 capture systems. Int J Greenhouse Gas Control 2015;39:377–89.
[46] Wu X, Shen J, Li Y, Wang M, Lawal A. Flexible operation of post-combustion solvent-based carbon capture for coal-fired power plants using multi-model predictive control: a simulation study. Fuel 2018;220:931–41.
[47] Wu X, Shen J, Li Y, Wang M, Lawal A. Nonlinear dynamic analysis and control design of a solvent-based post-combustion CO_2 capture process. Comput Chem Eng 2018;115:397–406.
[48] Feng G. A survey on analysis and design of model-based fuzzy control systems. IEEE Trans Fuzzy Syst 2006;14(5):676–97.
[49] Muske KR, Badgwell TA. Disturbance modeling for offset-free linear model predictive control. J Process Control 2002;12(5):617–32.
[50] Wu X, Shen J, Li Y, Lee KY. Fuzzy Modeling and Stable Model Predictive Tracking Control of Large-scale Power Plants. J Process Control 2014;24(10):1609–26.